Photoelectric Behavior of Sublimed Films of Phenothiazine Derivatives

Sadamu YOSHIDA, Kozo KOZAWA, Naoki SATO,† and Tokiko UCHIDA*
Department of Industrial and Engineering Chemistry, Faculty of Science and Technology, Science University of Tokyo, Noda, Chiba 278
† Institute for Chemical Research, Kyoto University, Uji, Kyoto 611
(Received December 15, 1993)

The energy structures and photoelectric behavior of sandwich-type organic photocells, configurations of which are Au/benzo[*b*]phenothiazine/Al, Al/dibenzo[*a,h*]phenothiazine/In, Al/dibenzo[*a,j*]phenothiazine/In, and Au/triphenodithiazine/Al, are investigated. The electrical and photovoltaic measurements show that the blocking contacts are formed at the pigments/Al interfaces in these four cells. These experimental results are consistent with the proposed energy band structures of the cells, which are estimated on the basis of the experimental results of ultraviolet photoelectron spectra and the threshold values in photocurrent action spectra.

Many works have published about photovoltaic cells made of organic pigments.[1—4] It is important for organic semiconductor films to study their energetic structure,[4—7] though there have not been many practical approaches.

In this paper, we try to estimate the electronic structure of phenothiazine derivative films on the basis of ultraviolet photoelectron spectrometric measurements, and to elucidate the photoelectric properties of these films by a band model.

Experimental

Materials. Seven phenothiazine (PT) derivatives, used in this work, are shown in Chart 1 with their abbreviations. They were prepared as described in the literature,[8—14] and purified by sublimation in vacuo. The metals used as electrodes for sandwich-type cells are aluminum, indium, and gold, the purity of which is better than 99.95%.

UP Spectra. Ionization potential and work functions of six PT derivatives, in the form of sublimed films on Cu substrates, were estimated by ultraviolet photoelectron spectrometry (UPS). Measurements were done by the method described in the literature.[15] The work function of metals, used for electrodes was also estimated by UPS. The UPS measurement for metal films was done after exposure to air for several minutes so as to put them in a similar condition to the cell electrodes.

Absorption Spectra. Electronic absorption (UV-vis) spectra of PT derivative films, sublimed on glass plates, were observed with a Hitachi 330 spectrometer.

X-Ray Measurements. The X-ray diffraction patterns of films were observed with a Rigaku CN 2013 diffractometer with a Mn-filtered Fe $K\alpha$ radiation (λ=1.9373 Å).

Cell Fabrication. To prepare thin-film sandwich-type cells, Pyrex glass plates (hereafter called substrates) were washed first with water and neutral detergent, then with high purity water, and finally by ultrasonic cleaning in isopropyl alcohol. Then they were dried and kept in a desiccator. Thin films, metal electrodes, and pigments, were vacuum-deposited onto substrates through a mask with a ULVAC EBH-6 at a base pressure of 10^{-5} Torr (1 Torr= 133.322 Pa). Figure 1 shows the arrangement of the films on a substrate. In some cells, where pigment/In was necessary, an Al layer was first deposited onto the glass plate as a conducting electrode, and then an In film was deposited, since the high resistance of semitransparent In film made the electrical measurements difficult. After the pigment was deposited onto the metal electrode (In), an Al layer completed the sandwich. In others, an Al layer was first deposited onto the glass plate, and then the pigment and Au were deposited successively. Metallic films were deposited so as to keep their transparency to more than 20% of the incident light. The substrate was kept at room temperature during sublimation, and the vacuum was broken after each deposition.

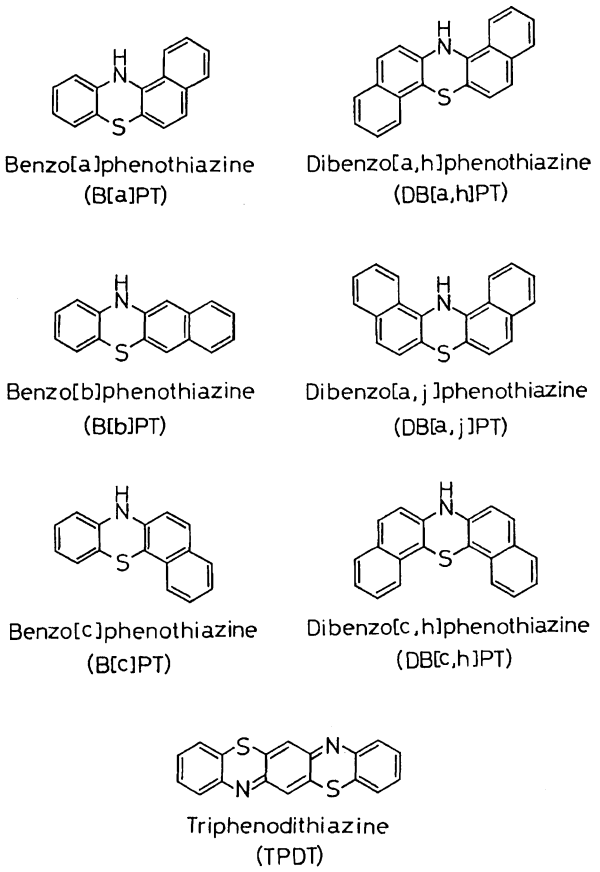

Chart 1. Molecular structures of PT derivatives.

Measurements. Electrical measurements on the cells were done in vacuo (10^{-5} Torr). The current–voltage (J–V) characteristics were observed with a Takedariken

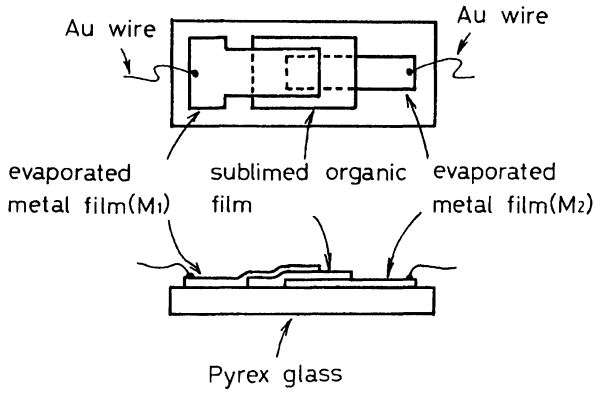

Fig. 1. Structure of a photoconductive cell prepared by vacuum evaporation.

TR8651 electrometer by biasing the cells with a Takedariken (Advantest) TR6142 function generator. For the photocurrent–voltage (J_p–V) measurements, cells were irradiated with a 750 W tungsten lamp, the intensity of which was measured with a Scientech laser power meter Model 360201. The action spectra of the sandwich-type cells were measured while keeping the photon flux constant throughout the wavelength range examined. The light source for action spectrum measurements was a 500 W xenon lamp and a JASCO CT-10 monochromator. The action spectra were normalized for the intensity of the incident light and were corrected for absorption of the glass plate. The thickness of film was measured by a Sloan Dektak 3030 surface profilometer.

Results and Discussion

Estimate of Band Structure. Figure 2 shows the estimated band structures of seven PT derivative films. In this figure, values of the top of the valence band and Fermi level are taken as those of ionization potential and work function, respectively, which are measured by UPS. The band gaps between the valence band and the conduction band are estimated from the energy of absorption threshold of the UV-vis spectra.

In looking at Fig. 2, all the PT derivative films, except for triphenodithiazine (TPDT) film, are regarded as p-type semiconductors, since their Fermi levels are below the centers of the band gaps. This estimation agrees with the fact that most organic pigments are known to have a p-type character.[5] It will be discussed in a later section if the models, estimated here, are proper or not together with the case of TPDT film estimated as n-type above.

Molecular Orientation of Films. X-Ray diffraction patterns of the films were observed to confirm that the molecular orientation in both films, used for UPS and electronic absorption measurements, were identical. For all the materials examined, similar X-ray patterns were observed for both films evaporated on Cu (UPS) and glass (UV-vis spectra) substrates with only one exception, the DB[*c,h*]PT film. In the case of DB[*c,h*]PT, a very weak diffraction peak appeared at around $2\theta=9.5°$ [(001) or (200)] with the film on a Cu substrate, but the film on glass substrate had amorphous patterns. It can be regarded that the energy structures of both organic films (on Cu and glass substrates) are identical. Figure 3 shows diffraction patterns of four PT derivative films. Benzo[*b*]phenothiazine (B[*b*]PT) and dibenzo[*a, h*]phenothiazine (DB[*a, h*]PT) films have distinct diffraction peaks, representing how the molecules are oriented in these films. On the other hand, there are no marked diffraction peaks in dibenzo[*a,j*]phenothiazine (DB[*a,j*]PT), and TPDT films. From the results of our preliminary X-ray crystal analysis,[17] the observed reflection peaks in B[*b*]PT film correspond to (*h*00) planes, and this means that the B[*b*]PT molecules stand perpendicularly on the substrate. However, assignment of the reflection peaks of DB[*a,h*]PT film was unsuccessful using the results of our X-ray crystal analysis, and it seems that orientation of DB[*a,h*]PT molecules in the sublimed film are different from that in single crystals.[18]

Energy Diagrams of the Cells. The notation (M_1/pigment/M_2) is used below to describe the sandwich-type cells used in this study. The order of symbols is the order of the films from the top of the assembly to the substrate.

It is well-known that a Schottky barrier is formed when a metal and a semiconductor, with different work functions, are brought into contact.[19] In this paper, combination of M_1, M_2, and pigments were selected by considering the band structure of pigments (Fig. 2) and values of the work function of metals, which were estimated by UPS, as 3.54, 4.00, and 4.50 eV, for Al, In, and Au, respectively.

Though this value of the work function for the Al film was smaller than the known value of 4.06—4.28 eV,[20] it can be attributable to the oxidized layer on the Al film surface.[21,22] By an electron take-off angle experiment of electron spectroscopy for chemical analysis (ESCA), Al_2O_3 (20 Å thick), and In_2O_3 (13 Å thick) layers have been found to be formed on the Al and In film surfaces. On the Au film surface, however, no oxidized layer was detected. In this connection, four kinds of materials, B[*b*]PT, DB[*a,h*]PT, DB[*a,j*]PT, and TPDT were adopted, and for each PT derivative, two electrodes were selected so that the one kept a rectifying contact, and the other formed an ohmic contact with the pigment. Then, Au/B[*b*]PT/Al, Al/DB[*a,h*]PT/In, Al/DB[*a,j*]PT/In, and Au/TPDT/Al cells were fabricated, and the thicknesses of the organic layers were 10000, 25000, 8500, and 10000 Å, respectively.

The estimated energy diagrams of these four cells are shown in Fig. 4. For the Au/B[*b*]PT/Al, Al/DB[*a,h*]PT/In, and Al/DB[*a,j*]PT/In cells, downward band bendings of pigments are formed at the interfaces with Al. On the other hand, at the interfaces with the opposite electrode, Au or In, band bendings of pigments are smaller than those at the interfaces with the Al electrode.

The band bendings presented in these diagrams sug-

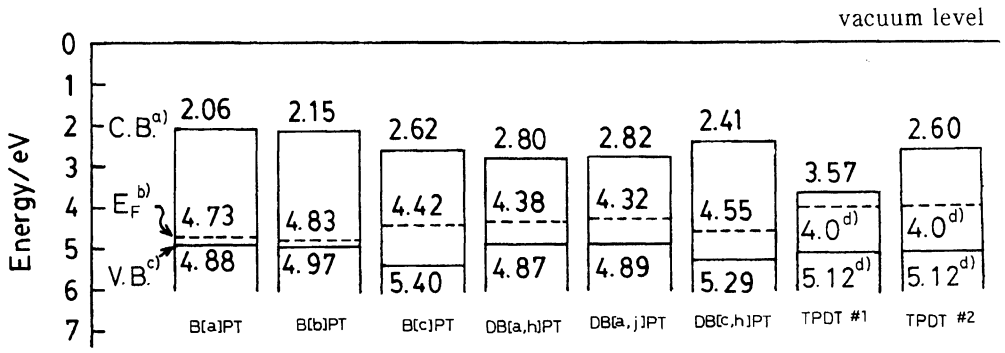

Fig. 2. Band structures of PT derivative films. Energy values are represented as depths from the vacuum level. Symbols are defined as follows: a) C.B.; bottom of conduction band, b) Fermi level, c) V.B.; top of valence band, and d) values taken from Ref. 16. TPDT #2 is explained in the text in the later section.

Table 1. Photovoltaic Characteristics of M_1/PT Derivative/M_2 Cells

Cell	V_{oc}/V	J_{sc}/A cm^{-2}	*f.f.*	η/%
Au/B[*b*]PT/Al	0.53	4.0×10^{-8}	0.38	6.7×10^{-7}
Al/DB[*a*,*h*]PT/In	0.50	1.0×10^{-8}	0.25	1.0×10^{-7}
Al/DB[*a*,*j*]PT/In	0.50	1.2×10^{-8}	0.25	1.3×10^{-7}
Au/TPDT/Al	0.24	2.3×10^{-8}	0.36	1.6×10^{-7}

gest that only the light absorbed near the Al contacts are effective in producing charge carriers, and that near ohmic contacts are formed at the Au or In contacts. In addition, the photocurrents generated are expected to flow from Al to Au or In through the pigment layers regardless of the direction of irradiation under short-circuit conditions.

In the case of the Au/TPDT/Al cell, the estimated energy diagram (Fig. 4(d)) is different from those of the other three cells. In this diagram, the upward band bending is formed at the Au/TPDT interface. This band bending suggests that the photoactive region is the Au/TPDT interface, and the photocurrent generated flows from Al to Au through the TPDT layer. A downward band bending is formed at the TPDT/Al interface, but this contact is assumed to be ohmic from the location of the bottom of the conduction band and the Fermi level.

All the estimated diagrams suggest that the cells show rectifying behavior in the dark, with a forward bias corresponding to a negative voltage at Al with respect to Au or In.

Dark Current. Figure 5 shows the observed dark current through the cells, J_d, as a function of the applied voltage, V. In the forward bias mode, the Al electrode was polarized negative with respect to the Au or In electrode. All cells showed some rectifying behavior, indicating that a Schottky barrier has formed. Figure 6 shows the semilogarithmic plots of the forward-biased dark current versus applied voltages for (a) the Au/B[*b*]-PT/Al cell and (b) the Au/TPDT/Al cell. The shape of these curves resembles that of the metal-insulator-semiconductor (MIS) barrier diode, as reported for an Al/SiO_2/p-type Si diode,[23] rather than that of the ideal Schottky barrier. Since the Al surface is easily oxidized to be covered with Al_2O_3 as mentioned above, the observed MIS characteristics can be explained by assuming that a pigment/Al_2O_3/Al diode is formed. These results are in accordance with the estimated band structure with respect to B[*b*]PT, but against to that with respect to TPDT, which is discussed in a later section.

Photocurrent. When the Au/TPDT/Al cell was irradiated on the Al side with white light of 1.2 W cm^{-2} intensity, it had a photovoltaic behavior as shown in Fig. 7. Other cells also had photovoltaic effects under the same conditions as the Au/TPDT/Al cell. And the Al electrode behaved as an anode in the short-circuit condition in all the cells examined; namely, the photocurrent flowed from Al to Au (or In) through the pigment layers regardless of the direction of irradiation. Since the irradiation on the Al side caused a larger photocurrent in these cells, the Schottky barriers are assumed to be formed at the pigment/Al interfaces.

From the J_p-V relationships in the photovoltaic mode, the characteristic photovoltaic parameters, open-circuit photovoltage, V_{oc}, short-circuit photocurrent, J_{sc}, fill factor, *f.f.*, and power conversion efficiency, η, can be evaluated. The results obtained for various cells are presented in Table 1. The very small values of η in Table 1 are probably caused by low carrier mobilities of the organic films.[24,25] In fact, we observed mobility values of 10^{-7}—10^{-5} cm^2 V^{-1} s^{-1} in PT-derivative films similar to those used in this paper.[26] Their very low conversion efficiency seems to make their practical application difficult.

Figure 8 shows the relationship between J_{sc} and the incident light intensity for the Au/B[*b*]PT/Al cell and the Au/TPDT/Al cell, irradiated through the Al side

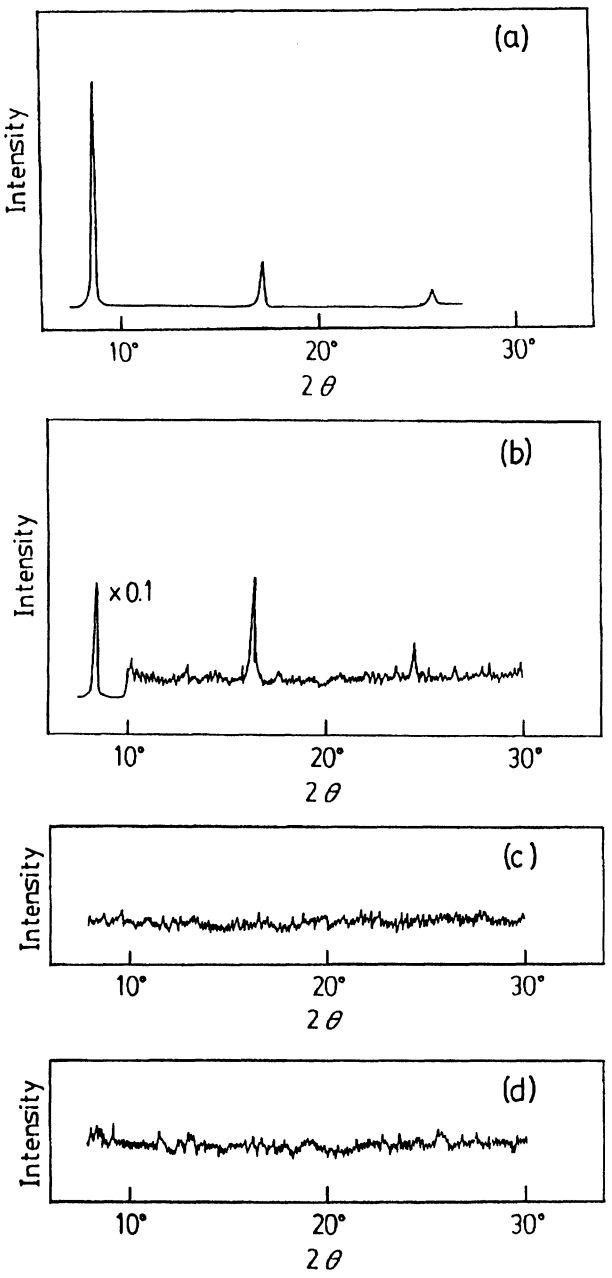

Fig. 3. X-Ray diffraction profiles of sublimed films of PT derivatives: (a) B[*b*]PT, (b) DB[*a*,*h*]PT, (c) DB-[*a*,*j*]PT, and (d) TPDT.

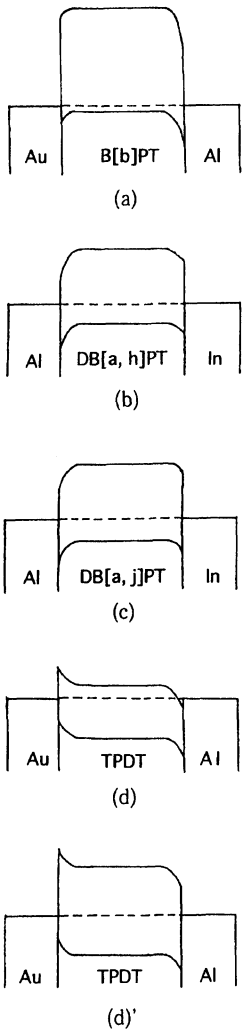

Fig. 4. Estimated energy diagrams of cells: (a) Au/B-[*b*]PT/Al, (b) Al/DB[*a*, *h*]PT/In, (c) Al/DB[*a*, *j*]-PT/In, and (d) Au/TPDT/Al cells. (d)′ is explained in the text in the later section.

with white light from a tungsten lamp, where the light intensity was varied from 80 to 1000 mW cm^{-2}. In both cases, values of J_{sc} are approximately proportional to the square root of the light intensities. For the Al/merocyanine/Ag and ITO/CdS/quinacridone/Au cell, a linear relationship between J_{sc} and light intensity has been reported.[27,28] The square root relation, which was observed in our cells, can be explained by electron-hole recombination.

Action Spectra. In Fig. 9, the photocurrent action spectra of M_1/pigment/M_2 cells illuminated through the M_1 and/or M_2 electrodes are shown together with absorption spectra of the corresponding organic films. The value of photocurrent has been normalized by the relative photon flux over the observed wavelength range.

For Au/B[*b*]PT/Al, Al/DB[*a*,*h*]PT/In, and Al/DB-[*a*, *j*]PT/In cells, the action spectra agree with the absorption spectra only when light is incident on the Al side. These results clearly indicate that photo-carriers are generated at the pigment/Al interfaces, that is, the Schottky barriers are formed at these regions. These results are consistent with the estimated energy diagrams mentioned in the previous section (Fig. 4(a)—(c)). For both Al/DB[*a*, *h*]PT/In and Al/DB[*a*,*j*]PT/In cells (Fig. 9(b) and (c)), illumination through the In sides gave small photocurrents, and the action spectra did not agree with their absorption spectra. These results can be explained by an optical filtering effect due to the absorption of light by the organic layers,[1,29] and these results indicate that no energy barrier is formed, neither at the DB[*a*,*h*]PT/In interface

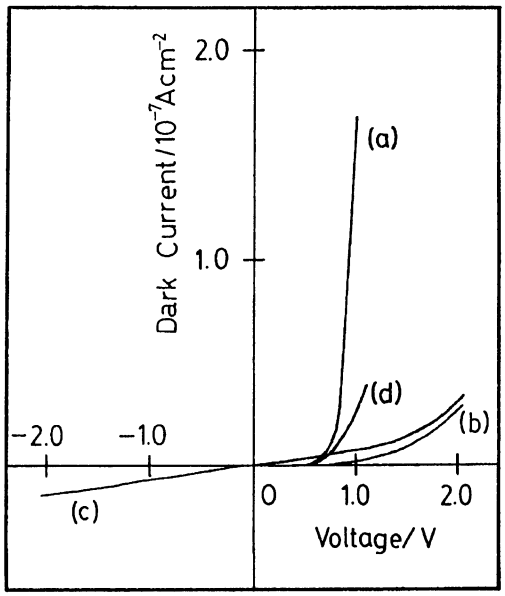

Fig. 5. Dark current–voltage characteristics: (a) Au/B[*b*]PT/Al, (b) Al/DB[*a,h*]PT/In, (c) Al/DB-[*a,j*]PT/In, and (d) Au/TPDT/Al cells.

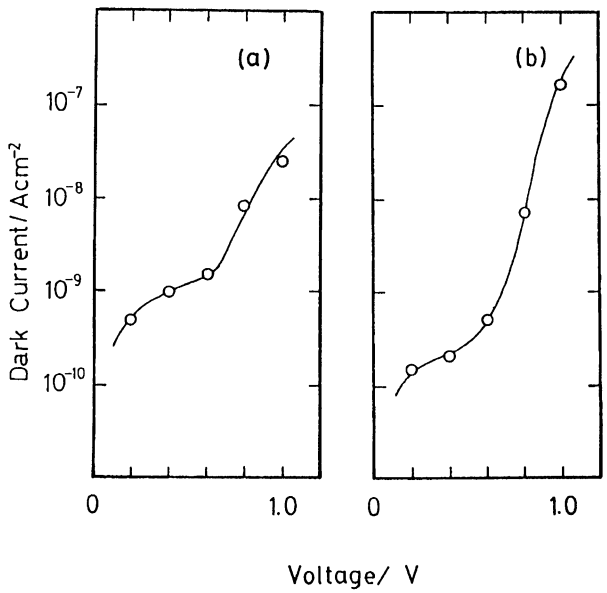

Fig. 6. Semilogarithmic plot of the forward dark current–voltage for (a) Au/B[*b*]PT/Al and (b) Au/TPDT/Al cells.

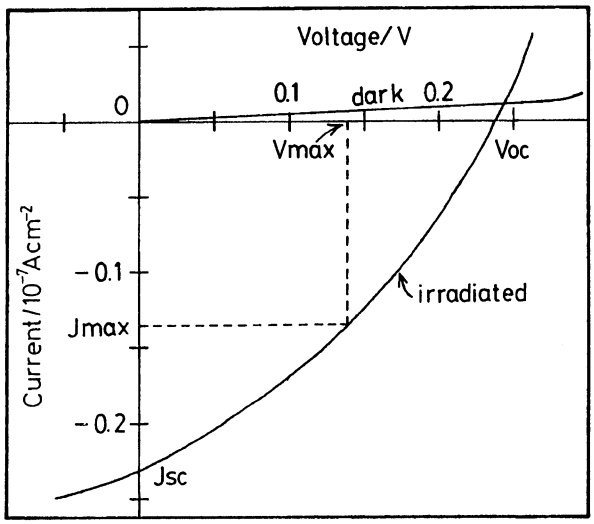

Fig. 7. Current–voltage characteristics of a Au/TPDT/Al cell under the white light. J_{max} and V_{max} are the current and voltage corresponding to the maximum power output.

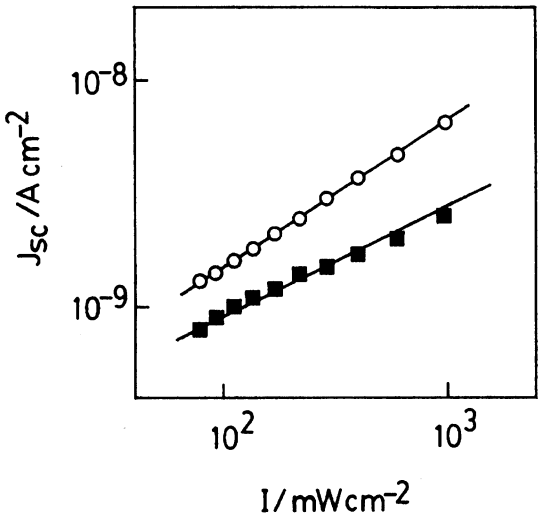

Fig. 8. Light intensity dependence of short-circuit photocurrent of the Au/B[*b*]PT/Al cell (—■—) and the Au/TPDT/Al cell (—○—).

nor the DB[*a,j*]PT/In interface. For the Au/B[*b*]PT/Al cell (Fig. 9(a)), when the Au side was illuminated, action spectrum gave a maximum around the absorption threshold of a B[*b*]PT film. This result also indicates that the energy barrier is not formed at the Au/B[*b*]-PT interface. In this case, however, the photocurrent value of the action spectrum obtained by the illumination through the Al side was much larger than that obtained by the illumination through the Au side around the absorption threshold of a B[*b*]PT film. This phenomenon cannot be explained only by the optical filtering effect, and may result from reexcitation of trapped carriers.

In the case of the Au/TPDT/Al cell, the results are somewhat different from the other three cells. When the Al electrode was irradiated, the action spectrum agreed with the absorption band around 300 nm of TPDT film. The action spectrum obtained from illuminating the Au electrode has a maximum around 380 nm, which is the trough of the two absorption bands of TPDT. These results are not consistent with the estimated energy diagrams (Fig. 4(d)), since the agreement between the action spectrum obtained from illuminating the Al side and the absorption band around 300 nm, indicates that the Schottky barrier is formed at the TPDT/Al interface. However, the action spectrum obtained by illu-

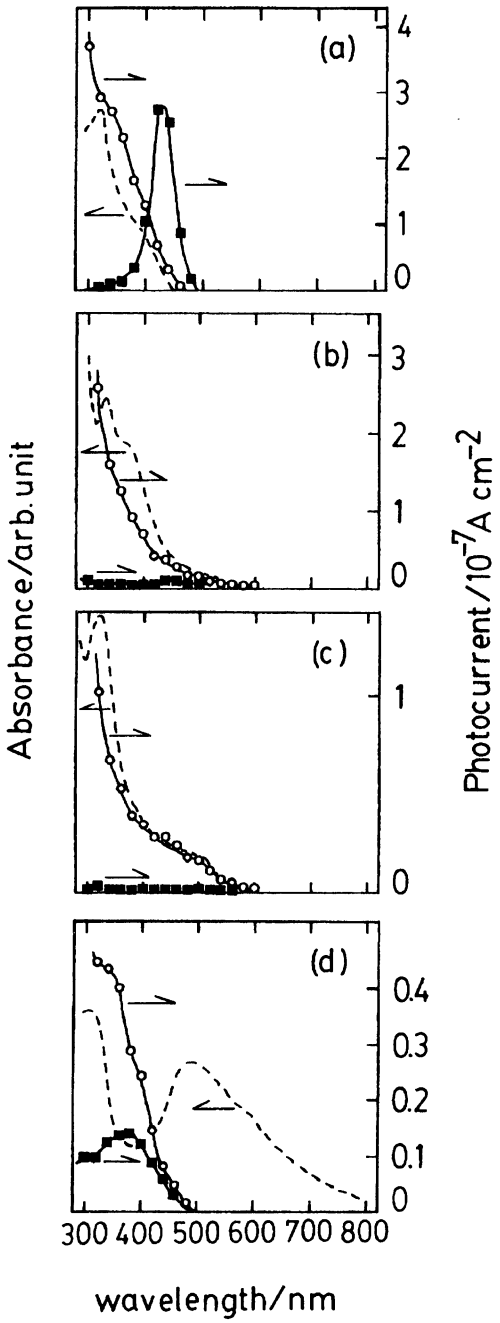

Fig. 9. Action spectra of cells for light incident on Al side (—○—), and Au or In side (—■—), and absorption spectra of vacuum deposited films of PT derivative (---): (a) Au/B[*b*]PT/Al, (b) Al/DB[*a,h*]-PT/In, (c) Al/DB[*a,j*]PT/In, and (d) Au/TPDT/Al cells.

minating the Au side was not very different from that obtained by illuminating the Al side. This result may be attributed to the occurrence of the charge separation at the Au/TPDT interface.

Neither action spectrum, by Al nor Au side irradiation, gives any peak that corresponds to the absorption band around 490 nm of TPDT film. Interpretation of these experimental results mentioned above can only be derived from the assumption that an exciton, formed in the absorption range around 490 nm, does not dissociate into an electron and a hole.

By applying this assumption, the band structure of TPDT in Fig. 2 (TPDT #1) should be corrected as given below, since the previous band gap was estimated from its absorption threshold (800 nm), in spite of having insufficient energy to produce charge carriers. Thus, the new band gap can be reestimated from the photovoltaic threshold (500 nm). The corrected band structure of TPDT film, and corrected energy diagram of the Au/TPDT/Al cell are shown in Fig. 2 (TPDT #2) and Fig. 4(d)′, respectively. The new band structure suggests that TPDT film is a p-type semiconductor. And in the new energy diagram, downward band bending is formed at the TPDT/Al interface, but upward band bending is formed at the Au/TPDT interface. The observed results about this cell, namely the J_d-V characteristic, direction of the short-circuit photocurrent, and the action spectra, are entirely explainable with the new energy diagram. In this diagram, the equal heights of energy barriers at both interfaces, Au/TPDT and TPDT/Al, perhaps make it difficult to elucidate the behavior of a photocurrent which is larger with the Al side irradiation than that on the other side. However, considering that the surface of an Al electrode is easily oxidized and covered with Al_2O_3 layer, the energy barrier at the TPDT/Al interface is possibly higher than that of the Au/TPDT interface.

For the other three cells, the absorption thresholds of the absorption spectra agree well with the threshold values of the action spectra. So, the observed photovoltaic behaviors of these cells agree with the estimated energy diagrams, shown in Fig. 2, without any correction.

The electrical properties of the cells mentioned above were measured in vacuo. In general, it is well known that the ambient gases, such as oxygen or hydrogen, influence the electrical behavior of organic materials.[30] In B[*b*]PT, DB[*a,h*]PT, and DB[*a,j*]PT films, the dark conductivity was observed to increase on oxygen adsorption, and to decrease on hydrogen adsorption. These effects of ambient gases on the dark conductivity show that these three materials have p-type properties which is in accordance with the estimated band structure shown in Fig. 2. However, neither oxygen nor hydrogen influenced the dark conductivity of TPDT film.

The conduction mechanism of organic compounds is usually explained either by a hopping model or by a band model. In this work, we could explain the observed photoelectric behaviors of PT derivative films by a band model with an energetical consideration, though the possibility of hopping conduction cannot be deleted for their low value of charge carrier mobility.[26]

We thank Mr. Toshiya Ishii of the Technical Research Institute of Toppan Printing Co., Ltd. for measurements of ESCA. We express our thanks to Mr. Norihiro

Uchida and Mr. Hiroshi Murashige for technical assistance.

References

1) A. K. Ghosh and T. Feng, *J. Appl. Phys.*, **49**, 5982 (1978).
2) H. J. Wagner, and R. O. Loutfy, *J. Vac. Sci. Technol.*, **20**, 300 (1982).
3) W. A. Nevin and G. A. Chamberlain, *J. Appl. Phys.*, **69**, 4324 (1991).
4) T. Tanaka and R. Hirohashi, *Nippon Kagaku Kaishi*, **1989**, 867.
5) M. Hiramoto, Y. Kishigami, and M. Yokoyama, *Chem. Lett.*, **1990**, 119.
6) T. Kawai, K. Tanimura, and T. Sakata, *Chem. Phys. Lett.*, **56**, 541 (1978).
7) K. Yamashita, Y. Harima, and Y. Matsumura, *Bull. Chem. Soc. Jpn.*, **58**, 1761 (1985).
8) E. Knoevenagel, *J. Pract. Chem.*, **89**, 14 (1914).
9) J. A. vanAllen, G. A. Reynolds, and R. E. Ader, *J. Org. Chem.*, **27**, 1659 (1962).
10) F. Kehrmann, A. Gressly, W. Chiffere, and M. Ramm, *Ber.*, **56B**, 649 (1923).
11) F. Kehrmann, *Ann.*, **322**, 51 (1902).
12) H. R. Snyder, *J. Am. Chem. Soc.*, **75**, 2015 (1953).
13) F. Kehrmann, *Chem. Ber.*, **55**, 2346 (1922).
14) J. Garbarczyk and A. Zuk, *Phosphorus Sulfur*, **6**, 351 (1979).
15) T. Hirooka, K. Tanaka, K. Kuchitsu, M. Fujihira, H. Inokuchi, and Y. Harada, *Chem. Phys. Lett.*, **18**, 390 (1973).
16) I. Shirotani, N. Sato, H. Nishi, K. Fukuhara, T. Kajiwara, and H. Inokuchi, *Nippon Kagaku Kaishi*, **1986**, 485.
17) Crystal data of B[*b*]PT are as follows: monoclinic, $P2_1/n$, $a=25.856(6)$, $b=7.838(2)$, $c=5.856(1)$ Å, $\beta=95.02(2)°$, $V=1183.7(7)$ Å^3, $Z=4$. X-Ray crystal structure analysis has not yet been complete because of a structural disorder (present $R=0.155$).
18) Crystal data of DB[*a*,*h*]PT are as follows: monoclinic, $P2_1/a$, $a=12.992(2)$, $b=9.430(2)$, $c=11.884(1)$ Å, $\beta=98.39(3)°$, $V=1440.2(9)$ Å^3, $Z=4$, $R=0.051$. The results of X-ray crystal structure analysis has not yet been published.
19) W. Schottky, *Z. Phys.*, **118**, 539 (1942).
20) H. B. Michaelson, *J. Appl. Phys.*, **48**, 4729 (1977).
21) E. E. Huber, Jr., and C. T. Kirk, Jr., *Surf. Sci.*, **5**, 447 (1966).
22) M. F. Lawrence, J. P. Dodelet, and L. H. Dao, *J. Phys. Chem.*, **88**, 950 (1984).
23) F. J. Kampas, K. Yamashita, and J. Fajer, *Nature*, **284**, 40 (1980).
24) Y. Shirota, *Kobunshi*, **38**, 346 (1989).
25) Y. Shirota, *Kagaku Kogyo*, **1984**, 790.
26) S. Yoshida, K. Kozawa, Y. Maruyama, and T. Uchida, *Bull. Chem. Soc. Jpn.*, **66**, 3548 (1993).
27) K. Kudo, S. Shiokawa, T. Moriizumi, K. Iriyama, and M. Sugi, *Denki Gakkai Ronbun Shi A*, **101**, 347 (1981).
28) K. Manabe, S. Kusabayashi, and M. Yokoyama, *Chem. Lett.*, **1987**, 609.
29) F-R. Fan and L. R. Faulkner, *J. Chem. Phys.*, **69**, 3341 (1978).
30) K. Yamashita, Y. Matsumura, Y. Harima, S. Miura, and H. Suzuki, *Chem. Lett.*, **1984**, 489.